

BEAM DYNAMICS STUDIES OF THE ELENA ELECTROSTATIC TRANSFER LINES

M.A. Fraser*, W. Bartmann, R. Ostojic, CERN, Geneva, Switzerland
 D. Barna, University of Tokyo, Tokyo, Japan

Abstract

The low-energy ELENA ring at the Antiproton Decelerator (AD) facility at CERN will lower the kinetic energy of antiproton beams from 5.3 MeV to 100 keV, significantly increasing the antiproton trapping efficiency at the experiments. The antiprotons from ELENA will be distributed to two experimental areas housing several different experiments through a system of electrostatic transfer lines totalling 90 m in length. A significant optimisation of the electrostatic optical elements (deflectors, quadrupoles, and correctors) has been carried out to improve the beam quality delivered to the experiments and facilitate installation of the beam lines into the AD hall. A general overview of the beam optics is presented, including end-to-end particle tracking and error studies from the extraction point in the ELENA ring to the experiments.

INTRODUCTION

The installation of the ELENA synchrotron [1] at CERN's AD facility will lower the kinetic energy of antiproton beams to 100 keV. A network of transfer lines has been designed to distribute the low energy antiproton beam to eight different experiments. The system is presently undergoing the first stage of installation in the AD hall. The layout of the transfer lines is shown in Fig. 1 and the relevant ELENA beam parameters for discussion in this paper are collected in Table 1. The transfer lines exploit electrostatic optical elements and are built up in a modular way from a series of standardised blocks: electrostatic quadrupole doublets with integrated correctors, beam position monitors, fast electric deflectors and electrostatic deflectors. After an initial optimisation of the orientation of the ELENA ring the transfer lines have been integrated and the geometry of the lines fixed in the AD hall. The fast deflectors located at each branch permit different bunches within the same bunch train extracted from ELENA to be distributed simultaneously to up to four experiments.

DESIGN OVERVIEW

The initial beam line design [2] was carried out using electrostatic beam line elements represented as transfer matrices and implemented in MADX [3]. The transfer matrices were computed by tracking test particles in the field maps generated using the finite element electromagnetic field solver COMSOL [4,5]. The higher-order (non-linear) field components were carefully optimised in each device as described elsewhere in these proceedings [6]. The design evolved in

several iterations, evaluating each time the effects of changes in the layout, or in the design of the optical elements, on the beam quality. The final validation of the transfer line design was achieved with end-to-end particle tracking in the field maps of all elements from the ELENA ring to the experiment, in the presence of errors and imperfections.

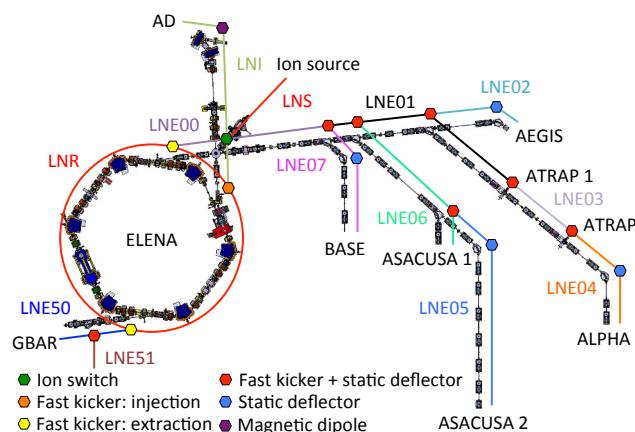


Figure 1: Layout of the ELENA transfer line network.

Table 1: ELENA Beam Parameters

Parameter	Injection	Extraction
Kinetic energy, W [MeV]	5.3	0.1
Reduced velocity, β	0.1064	0.0146
Magnetic rigidity [Gm]	3329	457
Electric rigidity [kV]	10570	200
No. of bunches	1	1 - 4
Emit. (95%) H/V [mm mrad]	< 15 / 15	6 / 4
Momentum spread (95%)	1×10^{-3}	2.5×10^{-3}
Intensity [\bar{p}]	3.0×10^7	1.8×10^7
Bunch length [m]	~ 12.7	1.3

The basic layout of the lines is determined by a FODO focusing structure with a cell length of 3.1 m and a phase advance of 90 deg per cell. The quadrupoles are housed in the same doublet assembly in order to standardise production; in the FODO sections only one of the quadrupoles in the assembly is powered, whereas in the matching sections both are powered.

Each doublet assembly contains separated horizontal and vertical correctors between the quadrupoles, giving two correctors per plane in each cell and good control over the beam trajectory. This is particularly important in areas where stray field from experimental equipment will play a role in beam tuning.

* mfraser@cern.ch

Content from this work may be used under the terms of the CC BY 3.0 licence (© 2015). Any distribution of this work must maintain attribution to the author(s), title of the work, publisher, and DOI.

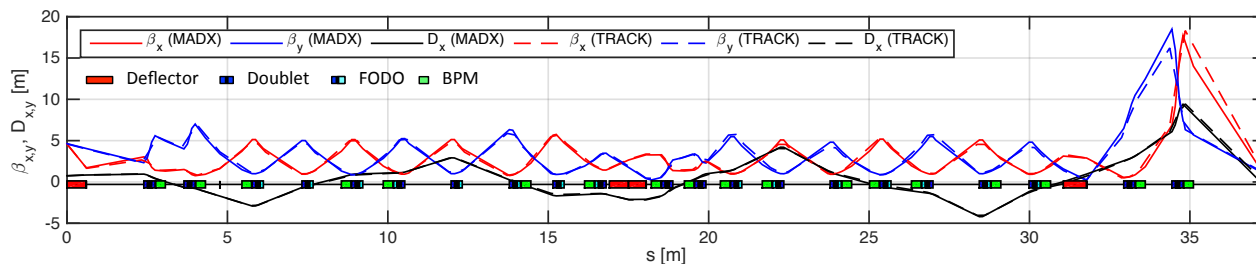


Figure 2: Optics functions from ELENA ring and ALPHA experimental target (left to right).

The beam position monitors (BPMs) are based on the secondary emission of electrons from a wire grid inserted into the beam. The BPM assembly is attached directly to each doublet wherever possible.

The FODO sections are interspersed with deflectors to switch between lines and matching sections to control the beam size through the deflectors and to focus the beam into the experiments. The transfer line optics is static and designed such that all lines can be matched simultaneously; each experiment will receive a bunch of antiprotons by programming the timing of the fast deflectors with a rise and fall time $< 1 \mu\text{s}$.

TRANSFER LINE BEAM OPTICS

The MADX model was used to perform the first-order matching and optimisation of the transfer lines. The TRACK [7] code was then used to assemble the 3D field maps exported from COMSOL and to track particles through the beam lines. TRACK applies Runge-Kutta methods to numerically integrate the 6D equations of motion of particles through arbitrary 3D, static or radio-frequency, electromagnetic field maps. The beam optics of the line to the ALPHA experiment, which is representative of the transfer line network as a whole, is used for demonstration purposes in this paper; the optics is summarised in Fig. 2, where the β -functions computed by MADX and TRACK are compared.¹ The small difference between the codes arises from the hard-edge approximation of the quadrupole fields applied in MADX and is most evident where the quadrupole strength is large. The simulation includes the lines LNE00, 01, 03 and 04 containing a fast extraction deflector, ~ 25 m of FODO beam line, another fast deflector and two static deflectors of 33.16 and 50.42 deg. The beam is matched from the ring to the first FODO section in LNE00 and LNE01, then matched through the fast switch to another FODO section where the beam proceeds through one more deflection before being matched to the experiment in LNE04. The beam size at ALPHA is optimised in the final matching section where the dispersion is also brought under control, reaching the beam size specification of 1 - 2 mm (FWHM). The change in bunch length along the transfer line is negligible.

The quadrupoles have an aperture of 60 mm between electrodes and the deflectors have an electrode gap of 65 mm.

¹ TRACK computes the Twiss parameters from a statistical analysis of the distribution of particles being tracked.

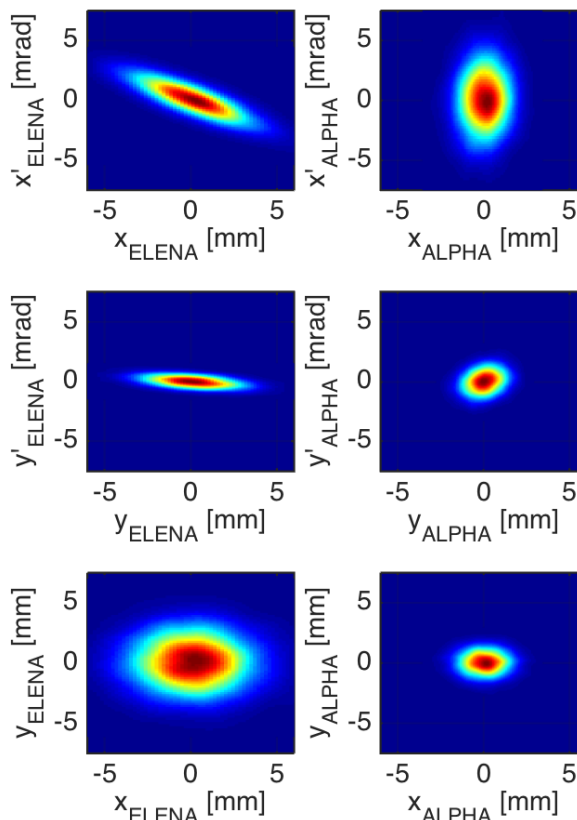


Figure 3: Phase space contour plots of tracked particle distribution from ELENA to ALPHA.

The acceptance of the line without steering errors or misalignment is 50 mm mrad, which is a factor 10 larger than the quoted nominal 95% transverse emittances at extraction from ELENA, and is limited by the large β -functions in the matching quadrupoles before the experiment. In the FODO sections the acceptance is almost 200 mm mrad.

The end-to-end tracking simulations validated the design guidelines used in the individual device optimisation, with less than 2% growth of the rms emittance coming from geometric aberrations in the nominal case without errors. This growth is negligible compared to the emittance growth driven by the non-zero dispersion along the line. The phase space at input and output to the tracking simulation is shown in Fig. 3, along with the beam spot at the ALPHA focal plane.

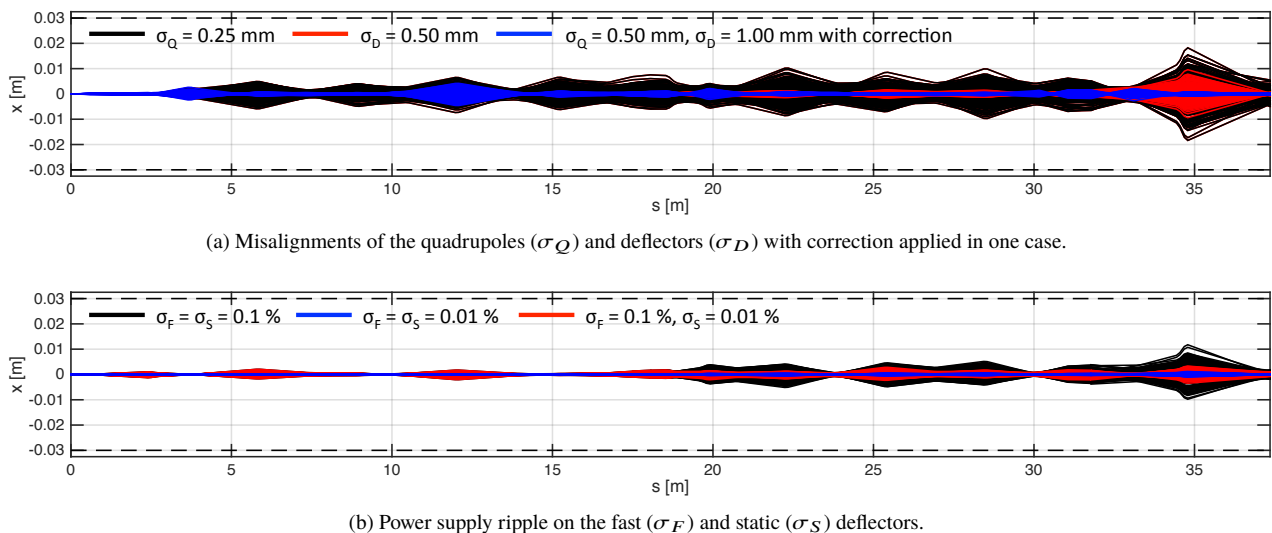


Figure 4: Error studies showing the beam trajectory for 200 random seeds along the transfer line to ALPHA.

ERROR STUDIES

Errors and imperfections were introduced in the simulations in order to specify the alignment tolerances and the voltage stability of the beam line elements, as well as to check the number of correctors, BPMs and their locations. The code comparison discussed above also permitted a benchmarking of the error and misalignment routines of the two codes. The first-order MADX model was found to be in very good agreement with tracking in perturbed and misaligned electrostatic field maps. All random errors were generated using a Gaussian distribution truncated at $\pm 3\sigma$, where σ is the standard deviation.

Misalignment and Trajectory Correction

The electrodes inside the vacuum tanks of the quadrupoles and deflectors will be aligned and passed through a metrological process in which their position will be measured with respect to fiducials placed on the outside of the tanks. The external reference points will be aligned in the AD hall using the metrology data such that the electrodes are placed on the nominal beam axis. For elements that are inside the same tank, and in cases where the adjacent element is rigidly attached, e.g. the fast and static deflectors, the misalignment errors are correlated. It is assumed that the experiments can help guide the steering of the beam into their experiment; in the case of ALPHA the trapping efficiency of the antiprotons is used as a figure of merit for the beam position at the experimental target.

Owing to the number of quadrupoles and their focusing strength, the transverse alignment of the quadrupoles (σ_Q) is more critical than the deflectors (σ_D). Uncorrected trajectories are shown in Fig. 4a for a $\sigma_Q = \pm 0.25$ mm random misalignment of the doublet tanks and $\sigma_D = \pm 0.5$ mm for the deflectors. Even rather large misalignments can be corrected effectively, as demonstrated for $\sigma_Q = \pm 0.5$ mm and $\sigma_D = \pm 1.0$ mm in Fig. 4a where the maximum corrector

strength required is 2.5 mrad. The larger trajectory excursion observed after ~ 12 m occurs in a region too congested to fit a BPM due to the close proximity of the switches to LNE06 and LNE07. The trajectory error after correction for $\sigma_Q = \pm 0.25$ mm and $\sigma_D = \pm 0.5$ mm has a negligible impact on the acceptance of the line. This is also the case with a BPM measurement accuracy of $\sigma = \pm 0.25$ mm.

Power Supply Stability

The effect of fast, uncorrectable jitter on the deflector voltages was simulated for relative errors of 0.01% and 0.1% on the fast (σ_F) and static (σ_S) deflectors, as shown in Fig. 4b. With a shot-to-shot jitter error of $\sigma_F = 0.1\%$ and $\sigma_S = 0.01\%$ the time-averaged rms horizontal emittance increase is 12% at the ALPHA experiment.

CONCLUSION

The ELENA transfer line layout and optics design was presented using the lines to the ALPHA experiment as a demonstration. Multi-particle tracking from ring to experiment using the 3D field maps of each active beam line component validated the design, and error studies specified the tolerances for misalignment and power supply stability. The first stage of installation has started in the AD hall with the installation of the LNS, LNI and LNE00 lines currently underway.

ACKNOWLEDGMENT

The authors would like to thank Brahim Mustapha (ANL) for his support during the implementation of the ELENA transfer lines in the TRACK beam dynamics code.

REFERENCES

- [1] V. Chohan (ed.), “Extra Low ENergy Antiproton (ELENA) ring and its Transfer Lines: Design Report,” CERN-2014-002, Geneva, Switzerland (2015).
- [2] G. Vanbavinckhove et al., “Geometry and Optics of the Electrostatic ELENA Transfer Lines” TUPWO051, *Proceedings of IPAC'13*, Shanghai, China (2013).
- [3] MADX website: <http://cern.ch/madx>
- [4] COMSOL website: <http://comsol.com>
- [5] D. Barna et al., “Field Simulations and Mechanical Implementation of Electrostatic Elements for the ELENA Transfer Lines” MOPRI101, *Proceedings of IPAC'14*, Dresden, Germany (2014).
- [6] D. Barna et al., “Design and Optimization of Electrostatic Deflectors for ELENA” MOPJE043, *These Proceedings, IPAC'15*, Richmond VA, USA (2015).
- [7] TRACK website:
<http://www.phy.anl.gov/atlas/TRACK/>